International Journal of Modern Physics B
Vol. 24, No. 9 (2010) 1079–1092

DOI: 10.1142/S0217979210055299

World Scientific
www.worldscientific.com

QUADRATURE SQUEEZING AND INFORMATION ENTROPY SQUEEZING IN NONLINEAR TWO-LEVEL SPIN MODELS

HORACIO GRINBERG*

Department of Physics, Facultad de Ciencias Exactas y Naturales, University of Buenos Aires, Pabellón 1, Ciudad Universitaria, (1428) Buenos Aires, Argentina
Consejo Nacional de Investigaciones Científicas y Técnicas, República Argentina
grinberg@df.uba.ar

Received 23 July 2009

Normal squeezing, variance and entropy squeezing factors based on the Heisenberg uncertainty principle and Shannon information entropy theory, respectively, derived from the entangled states of two-mode coherent states in two-photon processes are numerically investigated through a previously developed generalized nonlinear Jaynes–Cummings two-level spin model. Numerical simulations are performed and discussed for two two-photon model Hamiltonians in both resonant and off-resonant states of the spin system with the bimodal cavity field.

Keywords: Normal squeezing; variance squeezing; entropy squeezing; entanglement; two-level systems; two-mode interaction.

PACS numbers: 0365.Ca, 42.50.-p, 42.50.Ar, 42.50.Pq, 42.50.Dv, 89.70.Cf

1. Introduction

Nonlinear interactions leading to nonclassical effects of light play an essential role to entangle light or matter waves modes as, for instance, via spontaneous parametric down-conversion processes, multiwave mixing phenomena, or very intense laser–vacuum interactions.[1–5] There are mainly three phenomena that demonstrate the nonclassical character of light, that is, squeezing, photon antibunching, and sub-Poissonian photon statistics.[6–8]

Methods of nonlinear optics are mostly used to generate nonclassical light. Another possibility for generating the nonclassical state of light was proposed by Wodkiewicz *et al.* some time ago.[9] They find that the suitable superpositions of the vacuum and the one-photon or two-photon state may reduce the quantum

*Member of the Consejo Nacional de Investigaciones Científicas y Técnicas (CONICET), República Argentina.

fluctuations below the vacuum level. In fact, these superposition states can exhibit interesting nonclassical properties such as squeezing, higher-order squeezing, and sub-Poissonian photon statistics.[10] The emerging nonclassical properties are interpreted as due to the interference of the coherent states in phase space.[11] In particular, two-mode squeezed states, as nonclassical states of the two-mode light field, have also been much studied.[12] These squeezed states of light have been attractive for numerous applications since they have reduced quantum noise compared to that of coherent states.[13] One of the commonly used methods to generate squeezed light is optical parametric conversion and so far, a variety of methods have been proposed and demonstrated for the generation of squeezed states of light via this technique. Moreover, in Jaynes–Cummings models (JCM)[14] having three levels interacting with two modes of cavity fields, some nonclassical field states are also discovered in the system dynamics, even when the fields are assumed to be initially in two-mode coherent states.[15]

A light field where the variance of the number of photons is less than its mean is said to be sub-Poissonian or amplitude-squeezed. In this context, it is important to note that most of the studies of squeezing are based on the Heisenberg uncertainty relation, which is regarded as the standard limitation on measurements of quantum fluctuations. The Heisenberg uncertainty relation is formulated in terms of the variances of the system observables. These quantities are usually considered to be the most natural measures of the fundamental uncertainty associated with quantum fluctuations. The variances, containing only second-order statistical moments, however, are not an appropriate measure of the uncertainty in certain circumstances.[16] For example, if the variance, as the uncertainty measure for non-Gaussian states of the radiation field is used, one deliberately neglects higher-order statistical moments.[17] Similar problems with using the Heisenberg uncertainty relation have been pointed out and discussed in the past.[18–20]

An alternative definition of squeezing for the previously generalized JCM, based on Shannon information entropy theory, which overcomes the disadvantages of the definition based on the Heisenberg uncertainty relation was examined in the context of a two-level atom in the JCM as well as in resonance fluorescence.[16] More recently, the emerging concepts such as the purity, the entropy squeezing, and the variance squeezing were used to study statistical properties of a two-photon cavity mode in the presence of degenerate parametric amplifier.[21]

In the present paper, attention is concentrated on a class of two-mode nonclassical states associated to the dynamics of the field statistics and described via two-mode coherent states in two-photon processes. Specifically, the quantum noise associated with the second-order variance as well as the second-order Heisenberg variance and information entropy squeezing of these states, taken from the generalized nonlinear JCM previously developed by the author,[7,8,22] will be investigated. It will be shown that the previously uninvestigated squeezing phenomenon in this generalized nonlinear model can be partially generated for a wide range of model parameters, such as spin-field coupling constants, detuning parameters, mean pho-

ton numbers, etc. in both resonant and off-resonant states and in very short time intervals, on the picosecond time scale.

This paper is organized as follows. Section 2 briefly describes the two-level spin cyclic model used in the computations along with its interaction with a bimodal cavity field as well as the emerging quadrature squeezing and information entropy squeezing phenomena. In Sec. 3, the purity of the spin system, normal squeezing, and entropy and variance squeezing are discussed for two-model Hamiltonians in both resonant and off-resonant states of the two-level system with the cavity. Finally, Sec. 4 concludes the paper with a brief summary.

2. Theoretical Background

2.1. *Cyclic XY spin model*

In previous papers,[7,8,22–25] the XY n-spin cyclic model, as described by Lieb, Schultz, and Mattis[26] via the Hamiltonian

$$\mathcal{H}_\gamma(n^\dagger, n) = \sum_k \Xi_k \, n_k^\dagger \,, \quad n_k - \frac{1}{2} \sum_k \Xi_k \,, \tag{1}$$

was investigated by means of a functional integral representation involving nonorthogonal Grassmann (anticommuting) coherent states integration variables. In Eq. (1) $n^\dagger$, n are fermionic operators and the Ξ_k are the associated eigenvalues, given by

$$\Xi_k^2 = 1 - (1 - \gamma^2) \sin^2 k \,, \tag{2}$$

where γ is a parameter characterizing the degree of anisotropy in the xy-plane and where

$$k = 2\pi p/n \,, \quad p = -1/2n, \ldots, 0, 1, \ldots, 1/2n - 1 \,. \tag{3}$$

Use of the completeness relation of the n-site Grassmann states, invoking antiperiodic boundary conditions, performing an analytic continuation to Euclidean times, and the subsequent substitution $\Delta\tau/\hbar \to \beta$ ($\equiv 1/K_B T$) in the functional integral, allowed the imaginary time partition function of this model to be obtained as a configuration expansion through the trace formula for fermions. In this scenario, the energy of the model emerges as[23]

$$\Xi(n; \beta; \gamma) = -1/2 \sum_k \Xi_k - \frac{\partial}{\partial \beta} \ln \left(1 + \sum_{m=1}^{n} S(m) \right) , \tag{4}$$

where the mth configuration in the expansion becomes

$$S(m) = \sum_{\alpha_1 > \alpha_2 > \cdots > \alpha_m = 1} \prod_{j=1}^{m} \exp(-\beta \Xi_{\alpha_j}) \,. \tag{5}$$

Discussion of the sign of Ξ_k in Eq. (2) as well as the possibility of the existence of null eigenvalues are discussed in Refs. 24 and 25. In this paper, only positive

values of Ξ_k will be considered. This corresponds to a particle-hole picture for the n-particles, where the ground state has no elementary fermions and the elementary fermion excitations both above and below the Fermi surface have positive energies.[26]

2.2. *Interaction with a quantized cavity field*

The complete interaction picture Hamiltonian of a two-level system embedded in a two-mode cavity field and involving two-photon transitions can be written as $\mathcal{V}(t) = \lambda\mathcal{V}_1(t) + \mu\mathcal{V}_2(t)$, where the parameters λ and μ with λ, $\mu = 0$, 1, and $\lambda \neq \mu$ serve to define two different interacting Hamiltonians in the two-photon process involving diagonal and off-diagonal quadratic contributions of bosonic operators. Thus, invoking the rotating wave approximation[27] and after standard manipulations, the generalized nonlinear JCM Hamiltonians can be written as[7,8]

$$\mathcal{V}_1(t) = \hbar \sum_{j=1}^{2} g_j(\sigma_+ a_j^2 e^{i\Delta_j t} + a_j^{\dagger 2}\sigma_- e^{-i\Delta_j t}), \tag{6}$$

for $\lambda = 1$, $\mu = 0$, and

$$\mathcal{V}_2(t) = \hbar g(\sigma_+ a_1 a_2 e^{i\Delta t} + \sigma_- a_1^\dagger a_2^\dagger e^{-i\Delta t}), \tag{7}$$

for $\lambda = 0$, $\mu = 1$. The zero-point energy of the bosonic field was omitted and a constant term, given by $1/2(\omega_a + \omega_b)$, where ω_a and ω_b are the energies of the ground $|a\rangle$ and excited states $|b\rangle$, respectively, were ignored. $\sigma_\pm$, σ_z are the spin flip operators characterizing the effective two-level system, and $a_j^\dagger, a_j$ are bosonic creation and annihilation operators of cavity modes. In Eq. (6), g_j is the spin-field coupling constant for the mode j, and in Eq. (7), the coupling constant is given by $g = \sqrt{g_1 g_2}$. Δ_j and Δ are detuning parameters given by

$$\Delta_j \equiv \Delta_j(n;\beta;\gamma) = \sum_k \Xi_k + \Xi(n;\beta;\gamma) - 2\nu_j(\langle m_j\rangle;\beta), \tag{8}$$

and

$$\Delta = \sum_{k=1}^{2} \Xi_k + \Xi(n;\beta;\gamma) - (\nu_1(\langle m_1\rangle;\beta) + \nu_2(\langle m_2\rangle;\beta)), \tag{9}$$

for the interaction picture Hamiltonians (6) and (7) respectively. It is assumed that the field is in a thermal photon state in which $\nu_j(\langle m_j\rangle;\beta)$ is the photon frequency for the mode j, which can be expressed in terms of the mean photon number $\langle m_j\rangle$ in the two-mode cavity field through standard relations.[7,8,27]

Time evolution of the variance of the two-mode field quadrature operator emerging from the model Hamiltonians in Eqs. (6) and (7) was previously discussed in the context of correlated two-mode $SU(1,1)$ coherent states.[7,28]

It will be assumed that initially, the field modes are in coherent states $|\alpha_1\alpha_2\rangle$ and the spin system is in the excited state $|b\rangle$, i.e., the spin system and the field are

initially in a disentangled state while the time-dependent wavefunction evolves as

$$|\psi(t)\rangle = \sum_{n_1=0}^{\infty} \sum_{n_2=0}^{\infty} c_{n_1 n_2}(0) U(t) |b; n_1 n_2\rangle \,, \tag{10}$$

with the coefficients $c_{n_1 n_2}(0)$ given via density matrix elements at $t = 0$ in terms of the Poisson distribution

$$\rho_{n_i n_i}(0) = \frac{\langle n_i \rangle^{n_i} \, e^{-\langle n_i \rangle}}{n_i!} \,, \tag{11}$$

and where the spin system and the field are in an entangled state mediated by the unitary operator $U(t)$. Analytical expressions for the time-dependent density matrix for the case $\lambda = 1$, $\mu = 0$ were given in previous papers using Dyson perturbative expansion for the time evolution operator.[7,8,22] The same standard procedure applied to the case $\lambda = 0$, $\mu = 1$ leading to

$$\begin{aligned} \rho^{bb}_{n_1 n_2}(t) &= |\langle b; \, n_1 n_2 | \psi(t) \rangle|^2 \\ &= \rho_{n_1 n_1}(0) \rho_{n_2 n_2}(0) \left| 1 + g^2 (n_1 + 1)(n_2 + 1) \phi_2(t) \right|^2 , \end{aligned} \tag{12}$$

$$\begin{aligned} \rho^{aa}_{n_1 n_2}(t) &= |\langle a; \, n_1 n_2 | \psi(t) \rangle|^2 \\ &= \rho_{n_1 - 1 n_1 - 1}(0) \rho_{n_2 - 1 n_2 - 1}(0) \left| g \sqrt{n_1 n_2} \, \phi_1^*(t) + g^3 \sqrt{n_1^3 n_2^3} \, \phi_3^*(t) \right|^2 , \end{aligned} \tag{13}$$

and to

$$\rho^{bb}_{n_1 n_2}(t) = \rho_{n_1 n_1}(0) \rho_{n_2 n_2}(0) \cos^2 \left[\sqrt{(n_1 \, + \, 1)\,(n_2 \, + \, 1)} \, g t \right] , \tag{14}$$

$$\rho^{aa}_{n_1 n_2}(t) = \rho_{n_1 - 1 n_1 - 1}(0) \rho_{n_2 - 1 n_2 - 1}(0) \sin^2 \left[\sqrt{n_1 n_2} \, g t \right] , \tag{15}$$

for the diagonal matrix elements of $\rho_{n_1 n_2}(t)$ in the basis of spin states for the off-resonant ($\Delta \neq 0$) and resonant ($\Delta = 0$) states, respectively. It is observed that the trace of $\rho_{n_1 n_2}(t)$ over the ground $|a\rangle$ and excited $|b\rangle$ states of the spin system gives the photon distribution in the two-mode cavity. The time-dependent scalar functions $\phi_k(t)$ ($k = 1, 2, 3$) required in Eqs. (12) and (13) are given by[7,8]

$$\begin{aligned} \phi_1(t) &= \frac{1 - e^{i \Delta t}}{\Delta} \,, \\ \phi_2(t) &= \frac{e^{i \Delta t} - 1 - i t \Delta}{\Delta^2} \,, \\ \phi_3(t) &= \frac{2(e^{i \Delta t} - 1) - i t \Delta (1 + e^{i \Delta t})}{\Delta^3} \,. \end{aligned}$$

The associated off-diagonal elements of the density matrix in the space of the spin states are computed from

$$\begin{aligned} \rho^{ab}_{n_1 n_2}(t) &= \langle a; \, n_1 n_2 | \psi(t) \rangle \langle \psi(t) | b; \, n_1 n_2 \rangle \\ &= e^{i \Delta \phi_{n_1 n_2}} \sqrt{\rho^{aa}_{n_1 n_2}(t) \rho^{bb}_{n_1 n_2}(t)} \,, \end{aligned} \tag{16}$$

with $\rho^{ab}_{n_1n_2}(t) = \rho^{ba*}_{n_1n_2}(t)$ and where $\Delta\phi_{n_1n_2}$ is a phase determined by the real and imaginary parts of the time-dependent expansion coefficients emerging from Eq. (10).

Various nonclassical effects in the JCM can be generated by choosing different initial states of the field. For example, when the cavity field is initially in a coherent state of photons, one finds that the level occupation probability of the system can display collapse and revivals of the Rabi oscillations in a field that is not in a pure number state.[7,8,22,24,25]

2.3. *Quadrature operators, variances, and squeezing*

The field quadrature operators are defined as

$$X_1^{(i)}(t) = \frac{1}{2}(a_i(t) + a_i^\dagger(t))\,, \tag{17}$$

$$X_2^{(i)}(t) = \frac{1}{2i}(a_i(t) - a_i^\dagger(t))\,, \tag{18}$$

and their variances satisfy the uncertainty relation

$$\langle(\Delta X_1^{(i)})^2\rangle\langle(\Delta X_2^{(i)})^2\rangle \geq \frac{1}{16}\,, \tag{19}$$

which in turn means that if the equality holds at the zero-point, then each quadrature carries one-fourth of the quantum of the zero-point noise. In principle, the uncertainty relation in Eq. (19) allows the reduction of noise in one quadrature below the zero-point level with the amplification of noise in the other quadrature above the zero-point level. In other words, noise can be reduced below the zero-point level only by squeezing noise from one quadrature phase into the other. Thus, by definition, squeezing is said to exist whenever $\langle(\Delta X_j^{(i)})^2\rangle < (1/4)$ $(i, j = 1, 2)$. In order to characterize the influence of intrinsic decoherence on the squeezing, it was found it to be convenient to characterize the squeezing through the use of the modified[7] Mandel's Q parameter,[29] given by

$$Q_{ij} = 1 - 4\langle(\Delta X_j^{(i)})^2\rangle\,, \tag{20}$$

where $0 < Q_{ij} \leq 1$ for squeezing. The required expectation values of the normally ordered operators involved in Eq. (20) can be computed via density operator traces techniques as given elsewhere.[7]

2.4. *Entropy squeezing*

For a two-level system, characterized by the Pauli operators σ_x, σ_y, and σ_z, the Heisenberg uncertainty relation is given by

$$\Delta\sigma_i\Delta\sigma_j \geq |\langle\sigma_k\rangle|\epsilon_{ijk}\,, \tag{21}$$

where $\Delta\sigma = [\langle\sigma^2\rangle - \langle\sigma\rangle^2]^{1/2}$, with the commutation relations $\sigma \times \sigma = 2i\sigma$. Fluctuations in the component σ_i of the spin system (or the atomic dipole) are said to be squeezed if σ_i satisfies the condition

$$V(\sigma_i) = \Delta\sigma_i - |\langle\sigma_j\rangle|^{1/2} < 0\,, \quad i \neq j\,. \tag{22}$$

However, as claimed by Mao-Fa Fang *et al.*[16] the value of $\langle\sigma_i\rangle$ is highly dependent on the spin (or atomic) states used to perform the average, and may be zero for some states, in which case the uncertainty relation (21) is trivially satisfied (as $\Delta\sigma_i \geq 0$) and fails to provide any useful information. For example, for some states one can have $\langle\sigma_i\rangle = 0$, and therefore is not possible to obtain any information on squeezing from the inequality (21). Actually, these states may be considered to be maximally squeezed states of the spin system from the entropy point of view.

As an altenative to the Heisenberg uncertainty relation, several authors have studied quantum uncertainty by using quantum entropy theory, and obtained an entropic uncertainty relation for position and momentum which can overcome the limitations of the Heisenberg uncertainty relation. Moreover, the entropic uncertainty relation can be generalized to the case of two Hermitian operators in a K-dimensional Hilbert space and an optimal entropic uncertainty relation for sets of $K + 1$ complementary observables with nondegenerate eigenvalues in an even K-dimensional Hilbert space has been investigated.[19,20]

By defining

$$\delta H(\sigma_i) \equiv \exp[H(\sigma_i)]\,, \tag{23}$$

where $H(\sigma_i)$ is the Shannon information entropy, fluctuations in the component σ_i ($i \equiv x, y,$ or z) of the spin system are said to be "squeezed in entropy" if the information entropy $H(\sigma_i)$ of σ_i satisfies the condition

$$E(\sigma_i) = \delta H(\sigma_i) - \frac{2}{[\delta H(\sigma_k)]^{1/2}} < 0\,, \quad i \neq k\,. \tag{24}$$

In Sec. 3, the normal and entropy squeezing, based on the Heisenberg (variance) and on the entropic uncertainty relations, will be discussed through numerical simulations. It should be addressed that while the moment (variance) Heisenberg uncertainty relation is expressed as the *product* of the variances of two noncommutating observables A and B, the entropic uncertainty relation is given by the *sum* of their Shannon entropies.[16,21]

3. Results and Discussion

Squeezing phenomenon is one of the most interesting phenomena in the field of quantum optics. It reflects the nonclassical behavior for the quantum systems. In this section, numerical simultations of the normal, and the variance and entropy squeezing for the spin model system interacting with a two-mode cavity field in both resonant and off-resonant states will be discussed. The computations were conducted in the anisotropic limit $\gamma = 1$ assuming that the field is initially in a

coherent state and the spin system is in the excited state. In order to substantiate these results, we first examine the time evolution of purity of the whole system.

3.1. *Purity of the spin system*

The quantum state *purity* may be used as a good tool to give information about the entanglement of the components of the system (spin plus field). For this reason, this subsection will be devoted to discuss the purity of the system under consideration. The purity of the field can be determined from the quantity $Tr\rho^2(t)$. A necessary and sufficient condition for the ensemble to be described in terms of a pure state is that $Tr\rho^2(t) = 1$, in this case clearly a state vector description of each individual system of the ensemble is possible. For the case $Tr\rho^2(t) < 1$, the field will be in a statistical mixture state. However, for a two-level system, a maximally mixed ensemble corresponds to $Tr\rho^2(t) = 1/2$.[21,30] Thus, it follows from Eqs. (12)–(16) that

$$1/2 \leq Tr\rho^2(t) = 1 - 2\det\rho(t) \leq 1\,. \tag{25}$$

which provides the upper bound $\det\rho(t) \leq 1/4$. The analysis and discussion of the purity can be handled through Eq. (25). Thus, in Fig. 1, $Tr\rho^2(t)$ is plotted against t in the picosecond time scale, assuming that the field is prepared in a coherent state and the spin system is in the excited state. This figure displays the time evolution of the purity for a bimodal cavity field interacting with an effective two-level spin system for both interaction picture Hamiltonians (6) (solid curve) and (7) (dashed curve) in off-resonant [Fig. 1(a)] and resonant [Fig. 1(b)] states, respectively. We observe that the purity in general satisfies the inequalities $0.93 < Tr\rho^2(t) < 0.99$ in Fig. 1(a) and $0.50 < Tr\rho^2(t) < 0.99$ in Fig. 1(b). The system approaches the pure

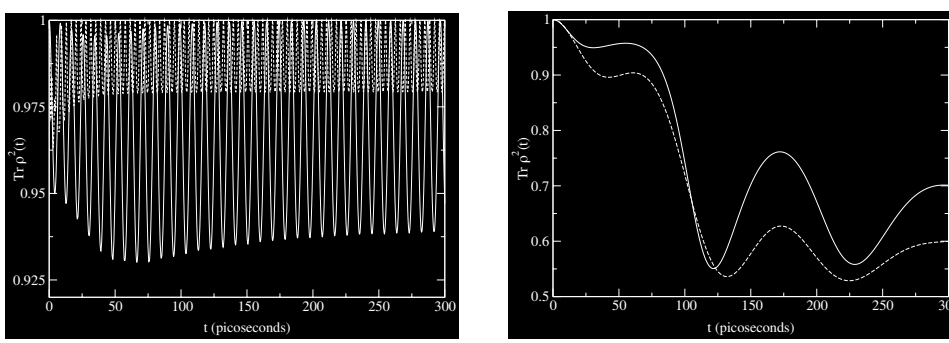

(a) (b)

Fig. 1. Time evolution of purity measured by $Tr\rho^2(t)$. The initial coherent state of the field is given by a Poisson distribution. (a) Solid curve: $\lambda = 1$, $\mu = 0$; $\langle n_1\rangle = 10$, $\langle n_2\rangle = 2$; $\Delta_1 = -22$ cm^{-1}, $\Delta_2 = -293$ cm^{-1}; $g_1 = 0.3$ cm^{-1}, $g_2 = 0.15$ cm^{-1}; dashed curve: $\lambda = 0$, $\mu = 1$; $\langle n_1\rangle = 36$, $\langle n_2\rangle = 20$; $\Delta = 56$ cm^{-1}; $g = 0.015$ cm^{-1}. (b) Solid curve: $\lambda = 1$, $\mu = 0$; $\langle n_1\rangle = \langle n_2\rangle = 30$; $\Delta_1 = \Delta_2 = 0$; $g_1 = 0.027$ cm^{-1}, $g_2 = 0.017$ cm^{-1}; dashed curve: $\lambda = 0$, $\mu - 1$; $\langle n_1\rangle = \langle n_2\rangle = 20$; $\Delta = 0$; $g = 0.05$ cm^{-1}.

state showing weak entanglement in Fig. 1(a) over the whole time scale considered. In the meantime, the maximum value of the purity becomes nearly 0.99. This means that the interaction between the field and the spin system is almost disentangled (at those times where the maximum value of $Tr\rho^2(t) = 0.99$). When $\Delta_1 = \Delta_2 = 0$ [solid curve in Fig. 1(b)] and $\Delta = 0$ [dashed curve in Fig. 1(b)] associated to the Hamiltonians (6) and (7), respectively, the behavior of the purity is strongly affected. In this case, the extrema (maxima and minima) of the purity function are decreased as compared to those observed in Fig. 1(a) but no fluctuations or interferences between patterns are detected. This means that the field becomes in a mixture state in Fig. 1(b), but without reaching its maximal, and therefore leads to a large enough entanglement for times longer than 75 ps. Also, it can be observed that the maximum value of the purity function in this case occurs at the onset of the interaction, and remains well above 0.9 for $t < 75$ ps. Here, it would be interesting to point out that although the maximum vale of $Tr\rho^2(t)$ does not reach the value *one* (pure state showing disentanglement), it is greater for the Hamiltonian (6) involving diagonal bosonic operators than for the Hamiltonian (7) where off-diagonal bosonic operators are involved. However, in contrast to the results shown in Fig. 1(a), in both cases, the interaction between the spin system and the field remains maximally correlated or entangled and, as a result of this interaction, the whole system never returns to the pure state. Thus, it is concluded that the diagonal and off-diagonal boson operators in the Hamiltonians (6) and (7), respectively, would affect the interaction between the field mode and spin system.

3.2. *Normal squeezing*

Squeezed light has less noise in one of the field quadratures than the vacuum level and an excess of noise in the other quadrature such that the Heisenberg uncertainty principle is satisfied. To discuss the phenomenon of squeezing, we use Eq. (20). The time evolution of the second-order quadrature variance $\langle(\Delta X_1^{(2)})^2\rangle$ was computed for various cases of interest and plotted in Fig. 2. We do notice that the time evolution does bring about noise reduction in this quadrature for both model Hamiltonians but with different degrees of squeezing. Thus, Fig. 2(a) shows a reasonable amount of squeezing, which is only lost at intervals around the maxima (solid curve). Squeezing can be observed for all t on the whole time scale considered when the Hamiltonian of Eq. (7) is used in the computation (dashed curve). When the value of the coupling constants is increased from 28 cm^{-1} in Fig. 2(a) to 61 cm^{-1} in Fig. 2(b), the squeezing is clearly observed for all t. We also notice that the Hamiltonian (6) [solid curves in Figs. 2(a) and 2(b)] generally gives an overall decrease in the level of noise as compared to the Hamiltonian (7), i.e., the reduction of noise is higher than that observed for the case $\lambda = 0$, $\mu = 1$. However, at certain intervals of time, the state associated to the Hamiltonian (6), becomes more classical as a result of the interaction with the two-photon JCM. This is particularly evident in Fig. 2(a) in the short time regime (below 12 ps), a result perhaps a little

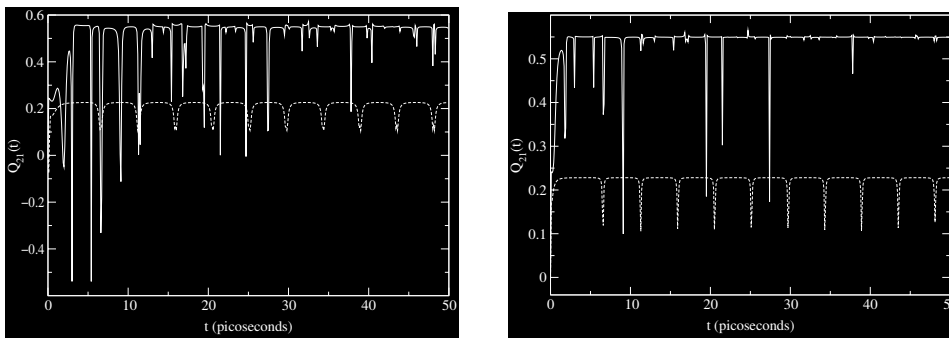

(a) (b)

Fig. 2. Time evolution of the normal second-order quadrature squeezing with the initial coherent state of the field given by a Poisson distribution. (a) Solid curve:: $\lambda = 1$, $\mu = 0$; $\langle n_1 \rangle = 4$, $\langle n_2 \rangle = 10$; $\Delta_1 = 41$ cm^{-1}, $\Delta_2 = 51$ cm^{-1}; $g_1 = g_2 = 28$ cm^{-1}; dashed curve: $\lambda = 0$, $\mu = 1$; $\langle n_1 \rangle = 4$, $\langle n_2 \rangle = 10$; $\Delta = 46$ cm^{-1}; $g = 28$ cm^{-1}; (b) same as (a) but with $g_1 = g_2 = 61$ cm^{-1}, $g = 61$ cm^{-1}.

surprising, since the form of the interaction would seem to preserve the correlations. The maximum magnitude of squeezing recovered in this nondegenerate state of the field is about 55% when the interaction picutre Hamiltonian of Eq. (6) is used (solid curve) while use of the Hamiltonian of Eq. (7) (dashed curve) leads to the same pattern of squeezing, about 20%, as that observed in Fig. 2(a). Thus, in off-resonant states, it is apparent that the value of the coupling constants plays an important role in determining the behavior of the second-order squeezing derived from the Hamiltonian of Eq. (6). Finally, computation of fourth-order squeezing, as given by Hong and Mandel[31] shows that the present model seems to give no evidence of such squeezing, at least in off-resonant states, for both interaction picture Hamiltonians (6) and (7), even for moderately large coupling constants and detuning parameters.

3.3. *Variance and entropy squeezing*

It is well-known that the entropy and variance squeezing are built up on the concept of the uncertainty relations in order to discuss the quantum fluctuations. The argument was to use the entropic uncertainty relations for two-level systems rather than the Heisenberg uncertainty relations used in the computations of normal squeezing. This has been discussed previously by a number of authors.[16,21] Frames (a) and (b) in Fig. 3 display the time evolution of the variance squeezing factor $V(\sigma_i)$ $(i = x, y)$ of both quadratures for the Hamiltonians (6) and (7), respectively, when the spin system is initially in the excited state. In Fig. 3(a) it is observed, according to Eq. (22), that squeezing mostly occurs in the second quadrature (σ_y) for times longer than 30 ps (dashed curve) when the Hamiltonian (6) is used. At very short times, the slow oscillations in the first quadrature σ_x below 30 ps only produce a small amount of squeezing (solid curve). However, use of Hamiltonian (7) in Fig. 3(b) shows that squeezing is present several times in the first quadrature at

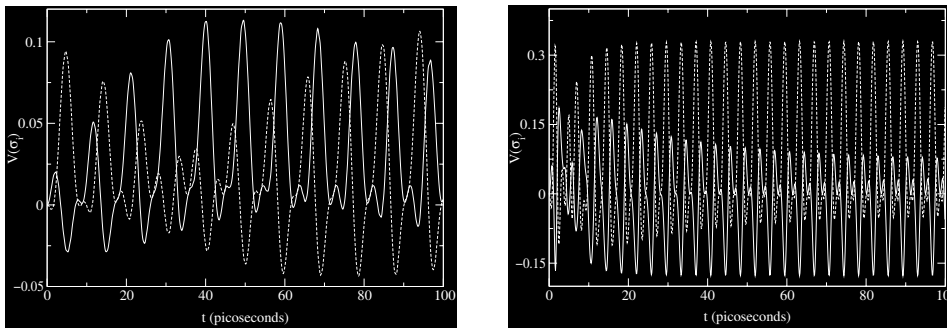

(a) (b)

Fig. 3. Time evolution of the based Heisenberg unceertainty relation variance squeezing factor $V(\sigma_i)$, with the initial coherent state of the field given by a Poisson distribution. (a) $\lambda = 1$, $\mu = 0$; $\langle n_1 \rangle = 10$, $\langle n_2 \rangle = 2$; $\Delta_1 = -22$ cm^{-1}, $\Delta_2 = -293$ cm^{-1}; $g_1 = 0.3$ cm^{-1}, $g_2 = 0.15$ cm^{-1}. Solid curve: $V(\sigma_x)$; dashed curve: $V(\sigma_y)$; (b) $\lambda = 0$, $\mu = 1$; $\langle n_1 \rangle = 36$, $\langle n_2 \rangle = 20$; $\Delta = 56$ cm^{-1}; $g = 0.015$ cm^{-1}. Solid curve: $V(\sigma_x)$; dashed curve: $V(\sigma_y)$.

regular intervals of time (solid curve) with the amplitudes approaching to the limit given by Eq. (22) in the long time regime. It is also observed that the amplitudes in the second quadrature (dashed curve) are more pronounced compared with those occurring in the first quadrature with the consequence that the squeezing tends to collapse as time goes on. Thus, Fig. 3 shows that although both $V(\sigma_x)$ and $V(\sigma_y)$ display squeezing effects in the two-level system, the variance squeezing factor provided by them is quite different. In particular, at the times scale $t \sim 3k\pi$ ps ($k = 1, 2, 3, \ldots$) in Fig. 3(a), the second quadrature $V(\sigma_y)$ exhibits larger variance squeezing for $k > 3$, while the first quadrature variance exhibits this behavior for $k < 3$. By contrast, both quadrature factors $V(\sigma_x)$ and $V(\sigma_y)$ in Fig. 3(b) show large fluctuations over the whole time scale, with a narrower separation between the peaks than that observed in Fig. 3(a). The resultant structure shows that squeezing can be significant for the first quadrature $V(\sigma_x)$, while the reduction in noise is lost for the second quadrature $V(\sigma_y)$ in the long time regime.

Figure 4 displays the time evolution of the entropy squeezing for various values of the coupling constant g in the Hamiltonian (7) in off-resonant [Fig. 4(a)] and resonant states [Figs. 4(b)–4(d)]. In Fig. 4(a), the squeezing occurs again several times in the first quadrature of the entropy squeezing $E(\sigma_x)$ (solid curve). The minima of this regular pattern remains constant over the whole time scale, and accounts for the 20% of the total squeezing. Thus, this is the optimal entropy squeezing factor in this particular case, i.e., the spin system has achieved a pure state at the times characterized by those minima. This entropy squeezing is practically absent from the second quadrature $E(\sigma_y)$ (dashed curve), except at short times (less than 40 ps). Figure 4(b) presents the entropy squeezing factor computed in the resonant state using the Hamiltonian (7) again. It is noted that there is an increase in the entropy squeezing amount in the second quadrature $E(\sigma_y)$ (dashed curve) as compared to

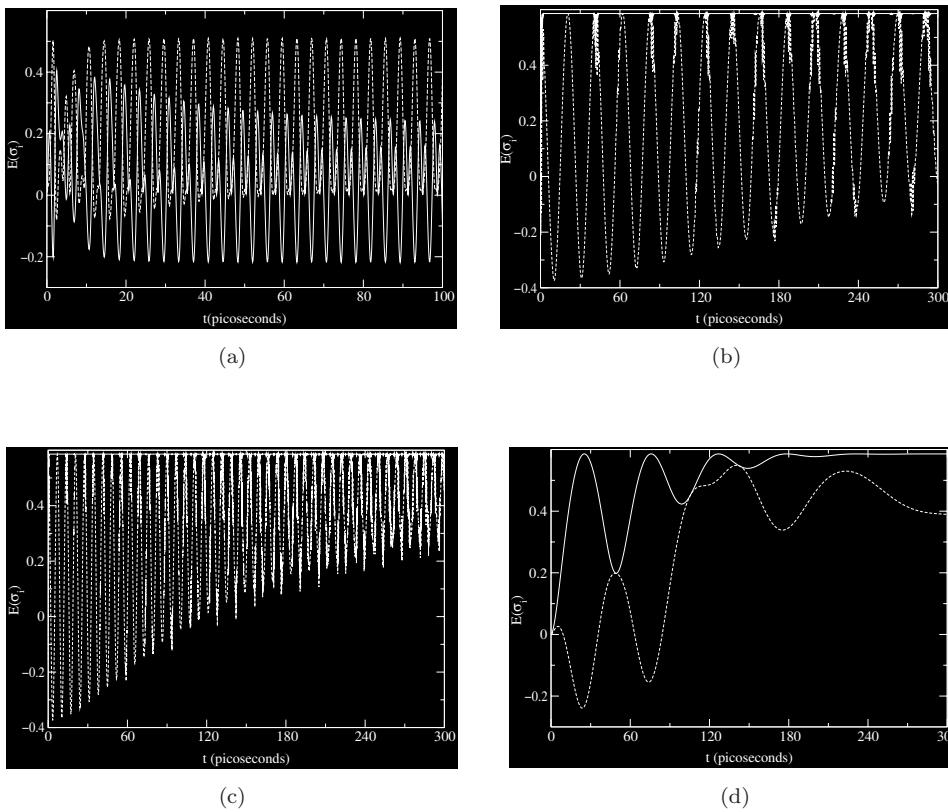

Fig. 4. Time evolution of the based Shannon information entropy squeezing factor $E(\sigma_i)$, with the initial coherent state of the field given by a Poisson distribution. (a) Same as Fig. 3(b). Solid curve: $E(\sigma_x)$; dashed curve: $E(\sigma_y)$; (b) $\lambda = 0$, $\mu = 1$; $\langle n_1 \rangle = \langle n_2 \rangle = 20$; $\Delta = 0$; $g = 5$ cm^{-1}. Solid curve: $E(\sigma_x)$; dashed curve: $E(\sigma_y)$; (c) same as (b) but with $g = 15$ cm^{-1}; (d) same as (b) but with $g = 0.05$ cm^{-1}.

that observed in Fig. 4(a), while no entropy squeezing is detected in the first quadrature $E(\sigma_x)$ (solid curve), in contrast to the result shown in Fig. 4(a). A comparison of the entropy squeezing factors in Figs. 4(b)–4(d) shows that with a decreasing of the coupling constant the quantum fluctuations are gradually suppressed and the peaks tend to separate. In fact, the "entropies" of any probabilistic distribution are well known to eliminate effectively the distance between peaks in the multipeak distributions. This is clearly seen in the transition from patterns in Figs. 4(b) and 4(d) to that in Fig. 4(c). At the same time, the growing coupling constant is accompanied by a substantial reduction in the entropy squeezing amount for the second quadrature $E(\sigma_y)$, with the result that no entropy squeezing is predicted for both quadratures above of 100 ps in the pattern of Fig. 4(c), where the coupling constant is larger than that in Figs. 4(b) and 4(d). The pattern of interferences with strong overlapping observed in Fig. 4(c) is consistent with an entangled state. Finally, with a coupling constant as small as 0.05 cm^{-1} in Fig. 4(d), there is no entropy squeezing

for the first quadrature $E(\sigma_x)$ while the second quadrature $E(\sigma_y)$ remains squeezed only below 80 ps, with the optimal entropy squeezing at around 28 ps. Again, this result stems from the fact that the spin system has achieved a pure state at this time, i.e., this state is just an eigenstate of the spin operator σ_y, displaying very weak entanglement, as predicted by the numerical simulation in Fig. 1(b), dashed curve.

4. Conclusion

The squeezing phenomenon derived from the interaction between a two-level spin system with a bimodal cavity field in a two-photon process was tackled. Two model interaction picture Hamiltonian involving quadratic terms in the field bosonic operators were separately analyzed and numerically discussed for a wide range of spin-field coupling constants, detuning parameters, and initial mean photon numbers. Numerical simulations for the time evolution of $Tr\rho^2(t)$ show that the system approaches the pure state with a very weak entanglement in off-resonant states for both Hamiltonians (6) and (7). In resonant states, it was found that the behavior of the purity is strongly affected, in this case with no detection of fluctuations or interferences between patterns. The field becomes in a mixture state and therefore leads to a large enough entanglement for times longer than 75 ps. Thus, the interaction between the spin system and the field remains maximally correlated or entangled in this case, and, as a result of this interaction, the whole system never returns to the pure state observed at the onset of the interaction. For very long times, the two-level system approaches to a maximally mixed ensemble which corresponds to $Tr\rho^2(t) = 1/2$.

Numerical calculations for normal second-order squeezing show a small amount of squeezing in resonant states, nevertheless, the pattern of interferences observed is consistent with an entangled state. In off-resonant states, there is a reasonable amount of squeezing for both Hamiltonians (6) and (7). However, no evidence was found of fourth-order squeezing in the present model.

In the present study, strong enhancement of quantum fluctuations in the variance squeezing based on the Heisenberg uncertainty relation as well as in entropy squeezing based on Shannon entropies which can be attributed to the complex interplay of quantum fluctuations and nonlinearities inherent to the model was detected. However, it was found that for the complex correlated quantum fluctuations associated with certain parameter region of the two-level spin system, the Shannon entropies could yield a more appropriate global description of squeezing than the entropy squeezing based on the Heisenberg uncertainty relation. Further investigation of the squeezing phenomenon in the present generalized nonlinear two-level spin model to elucidate the well known shortcomings of the variance measures of the Heisenberg uncertainties is underway and will be published elsewhere.

Acknowledgments

This work has been made possible by a research grant in aid from the Consejo Nacional de Investigaciones Científicas y Técnicas (PIP No 05098/08). The author is grateful to the reviewer for useful comments and to the Department of Physics, Facultad de Ciencias Exactas y Naturales, Universidad de Buenos Aires, for facilities provided during the course of this work.

References

1. D. N. Klyshko, *Photon and Nonlinear Optics* (Gordon and Breach Science Publishers, New York, 1989).
2. H. Xiong, M. O. Scully and M. S. Zubairy, *Phys. Rev. Lett.* **94**, 023601 (2005).
3. H. T. Tan, S. Zhu and M. S. Zubairy, *Phys. Rev. A* **72**, 022305 (2005).
4. S. Pielawa, G. Morigi, D. Vitali and L. Davidovich, *Phys. Rev. Lett.* **98**, 240401 (2007).
5. Y. I. Salamin, S. H. Hu, K. Z. Hatsagortsyan and C. H. Keitel, *Phys. Rep.* **427**, 41 (2006), and references therein.
6. C. C. Gerry and J. H. Eberly, *Phys. Rev. A* **42**, 6805 (1990).
7. H. Grinberg, *J. Phys. Chem. B* **112**, 16140 (2008).
8. H. Grinberg, *Int. J. Mod. Phys. B* **22**, 599 (2008).
9. K. Wodkiewicz, P. L. Knight, S. J. Buckle and S. M. Barnett, *Phys. Rev. A* **35**, 2567 (1987).
10. C.-L. Chai, *Phys. Rev. A* **46**, 7187 (1992).
11. W. Schleich, M. Pernigo and F. Le Kien, *Phys. Rev. A* **44**, 2172 (1991).
12. K. G. Köprülü, *J. Mod. Opt.* **55**, 1871 (2008).
13. H. J. Kimble and D. F. Walls, *J. Opt. Soc. Am. B* **4**, 1449 (1987).
14. E. T. Jaynes and F. W. Cummings, *Proc. IEEE* **51**, 89 (1963).
15. N. H. Abdel Wahab, *Phys. Scr.* **76**, 233 (2007).
16. M.-F. Fang, P. Zhou and S. Swain, *J. Mod. Opt.* **47**, 1043 (2000).
17. V. Bužek, C. H. Keitel and P. L. Knight, *Phys Rev. A* **51**, 2575 (1995).
18. K. Wodkiewicz and J. H. Eberly, *J. Opt. Soc. Am. B* **2**, 248 (1985).
19. J. Sánchez-Ruiz, *Phys. Lett. A* **201**, 125 (1995).
20. J. Sánchez-Ruiz, *Phys. Lett. A* **244**, 189 (1998).
21. M. Sebawe Abdalla, E. M. Khalil and A. S. F. Obada, *Ann. Phys.* **322**, 2554 (2007).
22. H. Grinberg, *Int. J. Quantum Chem.* **108**, 210 (2008).
23. H. Grinberg, *Phys. Lett. A* **311**, 133 (2003).
24. H. Grinberg, *Phys. Lett. A* **344**, 170 (2005).
25. H. Grinberg, *Phys. Lett. A* **350**, 428 (2006).
26. E. Lieb, T. Schultz and D. Mattis, *Ann. Phys.* **16**, 407 (1961).
27. S. M. Barnett and P. M. Radmore, *Methods in Theoretical Quantum Optics* (Oxford Science Publications, Oxford University Press Inc., New York, 1997).
28. C. C. Gerry and R. E. Welch, *J. Opt. Soc. Am. B* **9**, 290 (1992).
29. L. Mandel, *Phys. Rev. Lett.* **47**, 709 (1981).
30. More generally, $1/d \leq Tr\rho^2 \leq 1$ where d is the dimension of the Hilbert space attributed to the system it describes. See G. Jaeger, *Quantum Information. An Overview* (Springer, New York, 2007).
31. The $2N$th-order squeezing factor is given by $Q_{ij} = 1 - 2^N/(N-1)!! < (\Delta X_j^{(i)})^N >$, where $0 \leq Q_{ij} \leq 1$ for squeezing. See C. K. Hong and L. Mandel, *Phys. Rev. Lett.* **54**, 323 (1985).